PHYSICAL REVIEW D **86,** 071102(R) (2012)

Measurement of the $B_s^0 \to J/\psi \bar{K}^{*0}$ branching fraction and angular amplitudes

R. Aaij *et al.**
(LHCb Collaboration)

(Received 3 August 2012; published 8 October 2012)

A sample of 114 ± 11 $B_s^0 \to J/\psi K^- \pi^+$ signal events obtained with 0.37 fb^{-1} of pp collisions at $\sqrt{s} = 7$ TeV collected by the LHCb experiment is used to measure the branching fraction and polarization amplitudes of the $B_s^0 \to J/\psi \bar{K}^{*0}$ decay, with $\bar{K}^{*0} \to K^- \pi^+$. The $K^- \pi^+$ mass spectrum of the candidates in the B_s^0 peak is dominated by the $\bar{K}^{*0}$ contribution. Subtracting the nonresonant $K^- \pi^+$ component, the branching fraction of $B_s^0 \to J/\psi \bar{K}^{*0}$ is $(4.4^{+0.5}_{-0.4} \pm 0.8) \times 10^{-5}$, where the first uncertainty is statistical and the second is systematic. A fit to the angular distribution of the decay products yields the K^{*0} polarization fractions $f_L = 0.50 \pm 0.08 \pm 0.02$ and $f_\parallel = 0.19^{+0.10}_{-0.08} \pm 0.02$.

DOI: 10.1103/PhysRevD.86.071102 PACS numbers: 14.40.Nd, 13.25.Hw, 13.88.+e

Interpretations of measurements of time-dependent CP violation in $B_s^0 \to J/\psi \phi$ and $B_s^0 \to J/\psi f_0(980)$ decays have thus far assumed the dominance of the color-suppressed tree-level process. However, there are contributions from higher order (penguin) processes (see Fig. 1) that cannot be calculated reliably in QCD and could be large enough to affect the measured asymmetries. It has been suggested that the penguin effects can be determined by means of an analysis of the angular distribution of $B_s^0 \to J/\psi \bar{K}^*(892)^0$, where the penguin diagram is not suppressed relative to the tree-level one, and $SU(3)$ flavor symmetry arguments can be used to determine the hadronic parameters entering the $B_s^0 \to J/\psi \phi$ observables [1].

In this paper the $K^*(892)^0$ meson will be written as K^{*0}, while for other K^* resonances the mass will be given in parentheses. Furthermore, mention of any specific mode implies the use of the charge conjugated mode as well, and $K^- \pi^+$ pairs will be simply written as $K\pi$. The decay $B_s^0 \to J/\psi \bar{K}^{*0}$ has already been observed by the CDF experiment [2], which reported $\mathcal{B}(B_s^0 \to J/\psi \bar{K}^{*0}) = (8.3 \pm 3.8) \times 10^{-5}$. Under the assumption that the light quark (s, d) is a spectator of the b quark decay, the branching fraction can be approximated as

$$\mathcal{B}(B_s^0 \to J/\psi \bar{K}^{*0}) \sim \frac{|V_{cd}|^2}{|V_{cs}|^2} \times \mathcal{B}(B^0 \to J/\psi K^{*0}) = (6.5 \pm 1.0) \times 10^{-5}, \quad (1)$$

with $|V_{cd}| = 0.230 \pm 0.011$, $|V_{cs}| = 1.023 \pm 0.036$ [3], and $\mathcal{B}(B^0 \to J/\psi K^{*0}) = (1.29 \pm 0.05 \pm 0.13) \times 10^{-3}$ [4]. The measurement in Ref. [4], where the $K\pi$ S-wave contribution is subtracted, is used instead of the PDG average.

In this paper, 0.37 fb^{-1} of data taken in 2011 are used to determine $\mathcal{B}(B_s^0 \to J/\psi \bar{K}^{*0})$, to study the angular properties of the decay products of the B_s^0 meson, and to measure the resonant contributions to the $K\pi$ spectrum in the region of the K^{*0} meson. The measurement of the branching fraction uses the decay $B^0 \to J/\psi K^{*0}$ as a normalization mode.

The LHCb detector [5] is a single-arm forward spectrometer covering the pseudorapidity range $2 < \eta < 5$. The detector includes a high precision tracking system consisting of a silicon-strip vertex detector located around the interaction point, a large-area silicon-strip detector located upstream of a dipole magnet with a bending power of about 4 Tm, and three stations of silicon-strip detectors and straw drift tubes placed downstream. The combined tracking system has a momentum resolution $\Delta p/p$ that varies from 0.4% at 5 GeV/c to 0.6% at 100 GeV/c. Two ring-imaging Cherenkov detectors (RICH) are used to

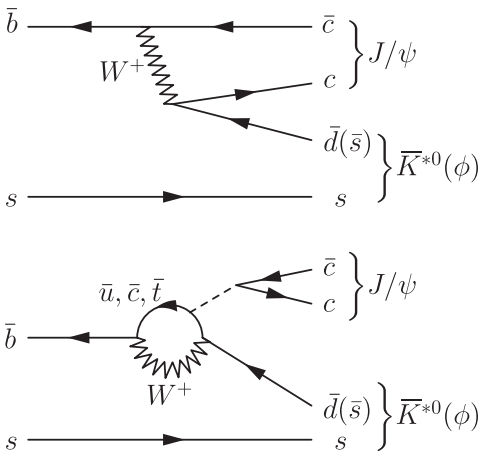

FIG. 1. Tree and penguin decay topologies contributing to the decays $B_s^0 \to J/\psi \bar{K}^{*0}$ and $B_s^0 \to J/\psi \phi$. The dashed line indicates a color singlet exchange.

*Full author list given at the end of the article.

determine the identity of charged particles. The separation of pions and kaons is such that, for efficiencies of ~75% the rejection power is above 99%. Photon, electron, and hadron candidates are identified by a calorimeter system consisting of scintillating-pad and preshower detectors, an electromagnetic calorimeter, and a hadronic calorimeter. Muons are identified by alternating layers of iron and multiwire proportional chambers.

The trigger consists of a hardware stage, based on information from the calorimeter and muon systems, followed by a software stage called high level trigger (HLT) that applies a full event reconstruction. Events with muon final states are triggered using two hardware trigger decisions: the single-muon decision (one muon candidate with transverse momentum $p_{\mathrm{T}} > 1.5$ GeV/c), and the di-muon decision (two muon candidates with $p_{\mathrm{T},1}$ and $p_{\mathrm{T},2}$ such that $\sqrt{p_{\mathrm{T},1} p_{\mathrm{T},2}} > 1.3$ GeV/c). All tracks in the HLT are required to have a $p_{\mathrm{T}} > 0.5$ GeV/c. The single-muon trigger decision in the HLT selects events with at least one muon track with an impact parameter IP > 0.1 mm with respect to the primary vertex and $p_{\mathrm{T}} > 1.0$ GeV/c. The dimuon trigger decision, designed to select J/ψ mesons, also requires a dimuon mass ($M_{\mu\mu}$) $2970 < M_{\mu\mu} < 3210$ MeV/c^2.

Simulated events are used to compute detection efficiencies and angular acceptances. For this purpose, pp collisions are generated using PYTHIA 6.4 [6] with a specific LHCb configuration [7]. Decays of hadronic particles are described by EVTGEN [8] in which final state radiation is generated using PHOTOS [9]. The interaction of the generated particles with the detector and its response are implemented using the GEANT4 toolkit [10] as described in Ref. [11].

The selection of $B^0_{(s)} \to J/\psi \overset{(-)}{K}{}^{*0}$ decays first requires the reconstruction of a $J/\psi \to \mu^+\mu^-$ candidate. The J/ψ vertex is required to be separated from any primary vertex (PV) by a distance-of-flight significance greater than 13. Subsequently, the muons from the J/ψ decay are combined with the K and π candidates to form a good vertex, where the dimuon mass is constrained to the J/ψ mass. A $p_{\mathrm{T}} > 0.5$ GeV/c is required for each of the four daughter tracks. Positive muon identification is required for the two tracks of the J/ψ decay, and the kaons and pions are selected using the different hadron probabilities based on combined information given by the RICH detectors. The candidate $B^0_{(s)}$ momentum is required to be compatible with the flight direction as given by the vector connecting the PV with the candidate vertex. An explicit veto to remove $B^+ \to J/\psi K^+$ events is applied, as they otherwise would pollute the upper sideband of the $B^0_{(s)}$ mass spectrum.

Following this initial selection, several geometrical variables are combined into a single discriminant geometrical likelihood variable (GL). This multivariate method is described in Refs. [12,13]. The geometrical variables chosen to build the GL are the $B^0_{(s)}$ candidate minimum impact parameter with respect to any PV in the event, the decay time of the $B^0_{(s)}$ candidate, the minimum impact parameter χ^2 of the four daughter tracks with respect to all PV in the event (defined as the difference between the χ^2 of the PV built with and without the considered track), the distance of closest approach between the J/ψ and K^{*0} trajectories reconstructed from their decay products, and the p_{T} of the $B^0_{(s)}$ candidate. The GL was tuned using simulated $B^0 \to J/\psi K^{*0}$ signal passing the selection criteria, and background from data in the $B^0_{(s)}$ mass sidebands with a value for the kaon particle identification variable in a range that does not overlap with the one used to select the data sample for the final analysis.

The $K\pi$ mass spectrum in the $B^0 \to J/\psi K\pi$ channel is dominated by the K^{*0} resonance but contains a non-negligible S-wave contribution, originating from $K^*_0(1430)^0$ and nonresonant $K\pi$ pairs [14]. To determine $\mathcal{B}(B^0_s \to J/\psi \bar{K}^{*0})$ it is therefore important to measure the S-wave magnitude in both $B^0_{(s)} \to J/\psi K\pi$ channels. The $K\pi$ spectrum is analyzed in terms of a nonresonant S-wave and several $K\pi$ resonances parametrized using relativistic Breit-Wigner distributions with mass-dependent widths, following closely [14]. The considered waves are a nonresonant S-wave amplitude interfering with the $K^*_0(1430)^0$ resonance, K^{*0} for the P wave, and $K^*_2(1430)^0$ for the D wave. F-wave and G-wave components are found to be negligible in the B^0 fit. In bins of the $K\pi$ mass, a fit is made to the $B^0_{(s)}$ candidate mass distribution to determine the yield. As shown in Fig. 2, a fit is then made to the B^0 and B^0_s yields as a function of the $K\pi$ mass without any efficiency correction. The S- and P-wave components dominate in the ± 40 MeV/c^2 window around the K^{*0} mass, where the K^{*0} contribution is above 90%. A more exact determination of this contribution using this method would require $K\pi$ mass-dependent angular acceptance corrections. For the branching fraction calculation, the fraction of K^{*0} candidates is determined from a different full angular and mass fit, which is described next.

The angular and mass analysis is based on an unbinned maximum likelihood fit that handles simultaneously the mass ($M_{J/\psi K\pi}$) and the angular parameters of the $B^0_{(s)}$ decays and the background. Each of these three components is modeled as a product of probability density functions (PDF), $\mathcal{P}(M_{J/\psi K\pi}, \psi, \theta, \varphi) = \mathcal{P}(M_{J/\psi K\pi})\mathcal{P}(\psi, \theta, \varphi)$, with ψ the angle between the kaon momentum in the rest frame of the K^{*0} and the direction of motion of the K^{*0} in the rest frame of the B. The polar and azimuthal angles (θ, φ) describe the direction of the μ^+ in the coordinate system defined in the J/ψ rest frame, where the x axis is the direction of motion of the $B^0_{(s)}$ meson, the z axis is normal to the plane formed by the x axis and the kaon momentum, and the y axis is chosen so that the y component of the kaon momentum is positive.

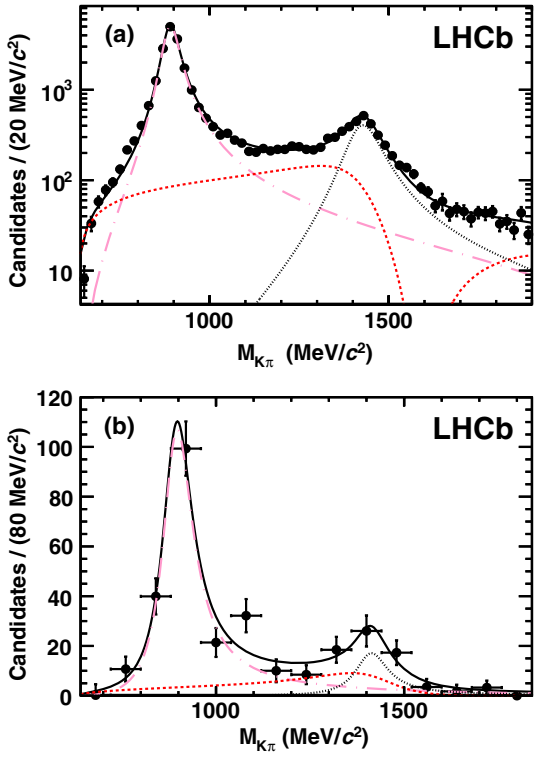

FIG. 2 (color online). Fit to the $K\pi$ mass spectrum for (a) $B^0 \to J/\psi K\pi$ events, and (b) $B_s^0 \to J/\psi K\pi$ events. The $B^0_{d(s)} \to J/\psi K\pi$ yields in each bin of the $K\pi$ mass are determined from a fit to the $J/\psi K\pi$ mass spectrum. The pink dashed-dotted line represents the K^{*0}, the red short-dashed line is the S-wave, and the black dotted line is the $K_2^*(1430)$. The black solid line is their sum.

The function describing the mass distribution of both $B^0_{(s)}$ signal peaks is the sum of two crystal ball (CB) functions [15], which are a combination of a Gaussian and a power law function to describe the radiative tail at low masses,

$$\mathcal{P}(M_{J/\psi K\pi}) = f\mathrm{CB}(M_{J/\psi K\pi}, \mu_B, \sigma_1, \alpha_1) + (1-f)\mathrm{CB}(M_{J/\psi K\pi}, \mu_B, \sigma_2, \alpha_2). \quad (2)$$

The starting point of the radiative tail is governed by a transition point parameter $\alpha_{(1,2)}$. The mean and width of the Gaussian component are μ_B and $\sigma_{(1,2)}$. The values of the f, σ_1, σ_2, α_1, and α_2 parameters are constrained to be the same for the B_s^0 and B^0 peaks. The difference in the means between the B_s^0 and the B^0 distributions, $(\mu_{B_s^0} - \mu_{B^0})$, is fixed to the value taken from Ref. [16]. The mass PDF of the background is described by an exponential function.

Assuming that direct CP violation and the $B^0_{(s)} - \bar{B}^0_{(s)}$ production asymmetry are insignificant, the differential decay rate is [1,17]

$$\begin{aligned}\frac{\mathrm{d}^3\Gamma}{\mathrm{d}\Omega} \propto\ & 2|A_0|^2\cos^2\psi(1-\sin^2\theta\cos^2\varphi) \\ & + |A_\parallel|^2\sin^2\psi(1-\sin^2\theta\sin^2\varphi) + |A_\perp|^2\sin^2\psi\sin^2\theta \\ & + \frac{1}{\sqrt{2}}|A_0||A_\parallel|\cos(\delta_\parallel-\delta_0)\sin 2\psi\sin^2\theta\sin 2\varphi \\ & + \frac{2}{3}|A_S|^2[1-\sin^2\theta\cos^2\varphi] \\ & + \frac{4\sqrt{3}}{3}|A_0||A_S|\cos(\delta_S-\delta_0)\cos\psi[1-\sin^2\theta\cos^2\varphi] \\ & + \frac{\sqrt{6}}{3}|A_\parallel||A_S|\cos(\delta_\parallel-\delta_S)\sin\psi\sin^2\theta\sin 2\varphi, \end{aligned} \quad (3)$$

where A_0, $A_\parallel$, and $A_\perp$ are the decay amplitudes corresponding to longitudinally and transversely polarized vector mesons. $A_S = |A_S|e^{i\delta_S}$ is the $K\pi$ S-wave amplitude and $(\delta_\parallel - \delta_0)$ the relative phase between the longitudinal and parallel amplitudes. The convention $\delta_0 = 0$ is used hereafter. The Ω differential is $\mathrm{d}\Omega \equiv \mathrm{d}\cos\psi\,\mathrm{d}\cos\theta\,\mathrm{d}\varphi$. The polarization fractions are normalized according to

$$f_{L,\parallel,\perp} = \frac{|A_{0,\parallel,\perp}|^2}{|A_0|^2 + |A_\parallel|^2 + |A_\perp|^2}, \quad (4)$$

which satisfy $f_L + f_\parallel + f_\perp = 1$.

The parameters f_L, $f_\parallel$, and $\delta_\parallel$ describing the P wave are left floating in the fit. The $|A_S|$ amplitude and the δ_S phase depend on $M_{K\pi}$, but this dependence is ignored in the fit, which is performed in a $K\pi$ mass window of ± 40 MeV$/c^2$, and they are just treated also as floating parameters. A systematic uncertainty is later associated with this assumption. The angular distribution of observed events is parametrized as a product of the expression in Eq. (3) and a detector acceptance function, $\mathrm{Acc}(\Omega)$, which describes the efficiency to trigger, reconstruct, and select the events. Simulation studies have shown almost no correlation between the three one-dimensional angular acceptances $\mathrm{Acc}_\psi(\psi)$, $\mathrm{Acc}_\theta(\theta)$, and $\mathrm{Acc}_\varphi(\varphi)$. Therefore, the global acceptance factorizes as $\mathrm{Acc}(\Omega) = \mathrm{Acc}_\psi(\psi)\mathrm{Acc}_\theta(\theta)\mathrm{Acc}_\varphi(\varphi)$, where $\mathrm{Acc}_\psi(\psi)$ is parametrized as a fifth degree polynomial, $\mathrm{Acc}_\theta(\theta)$ as a second degree polynomial, and $\mathrm{Acc}_\phi(\phi)$ as a sinusoidal function. A systematic uncertainty due to this factorization hypothesis is later evaluated. The angular distribution for the background component is determined using the upper sideband of the B_s^0 mass spectrum, defined as the interval $[5417, 5779]$ MeV$/c^2$.

Figure 3 shows the projection of the fit in the $M_{J/\psi K\pi}$ mass axis, together with the projections in the angular variables in a window of ± 25 MeV$/c^2$ around the B_s^0 mass. The number of candidates corresponding to B^0 and B_s^0 decays is found to be $13,365 \pm 116$, and 114 ± 11, respectively.

Tables I and II summarize the measurements of the $B^0_{(s)} \to J/\psi K^{(-)*0}$ angular parameters, together with their statistical and systematic uncertainties. The correlation coefficient given by the fit between f_L and $f_\parallel$ is $\rho = -0.44$ for B^0_s decays. The results for the $B^0 \to J/\psi K^{*0}$ decay are in good agreement with previous measurements [4,15,18,19]. Based on this agreement, the systematic uncertainties caused by the modeling of the angular acceptance were evaluated by summing in quadrature the statistical error on the measured $B^0 \to J/\psi K^{*0}$ parameters with the uncertainties on the world averages ($f_L = 0.570 \pm 0.008$ and $f_\perp = 0.219 \pm 0.010$) [3]. The angular analysis was repeated with two additional acceptance descriptions, one which uses a three-dimensional histogram to describe the efficiency avoiding any factorization hypothesis, and another one based on a method of normalization weights described in Ref. [19]. A very good agreement was found in the values of the polarization fractions computed with all the three methods. For the parameter $|A_S|^2$, uncertainties caused by the finite size of the simulation sample used for the acceptance description, as well as from the studies with several acceptance models, are included. The systematic uncertainty caused by the choice of the angular PDF for the background is shown for the $B^0_s \to J/\psi \bar{K}^{*0}$ decay but it was found to be negligible for $B^0 \to J/\psi K^{*0}$.

Also included in Tables I and II is the uncertainty from the assumption of a constant δ_S as a function of $M_{K\pi}$. This assumption can be relaxed by adding an extra free parameter to the angular PDF. This addition makes the fit unstable for the small size of the B^0_s sample but can be used in the control channel $B^0 \to J/\psi K^{*0}$. The differences found in the B^0 parameters with the two alternate parametrizations are used as systematic uncertainties. The parameters $\delta_\parallel$ fit to $\cos(\delta_\parallel) = -0.960^{+0.021}_{-0.017}$ for the B^0 and to $\cos(\delta_\parallel) = -0.93 \pm 0.31$ (where the error corresponds to the positive one, being symmetrized) for the B^0_s. These parameters could in principle affect the efficiency corrections, but it was found that the effect of different values of $\delta_\parallel$ on the overall efficiency is negligible. A simulation study of the fit pulls has shown that the errors on f_L and $f_\parallel$ of the B^0_s decays are overestimated by a small amount ($\sim 10\%$) since they do not follow exactly a Gaussian distribution; therefore, the decision was taken to quote an uncertainty that corresponds to an interval containing 68% of the generated experiments, rather than giving an error corresponding to a log-likelihood interval of 0.5. A slight bias observed in the pulls of $f_\parallel$ in B^0_s decays was accounted for by adding a systematic uncertainty corresponding to 6% of the statistical error.

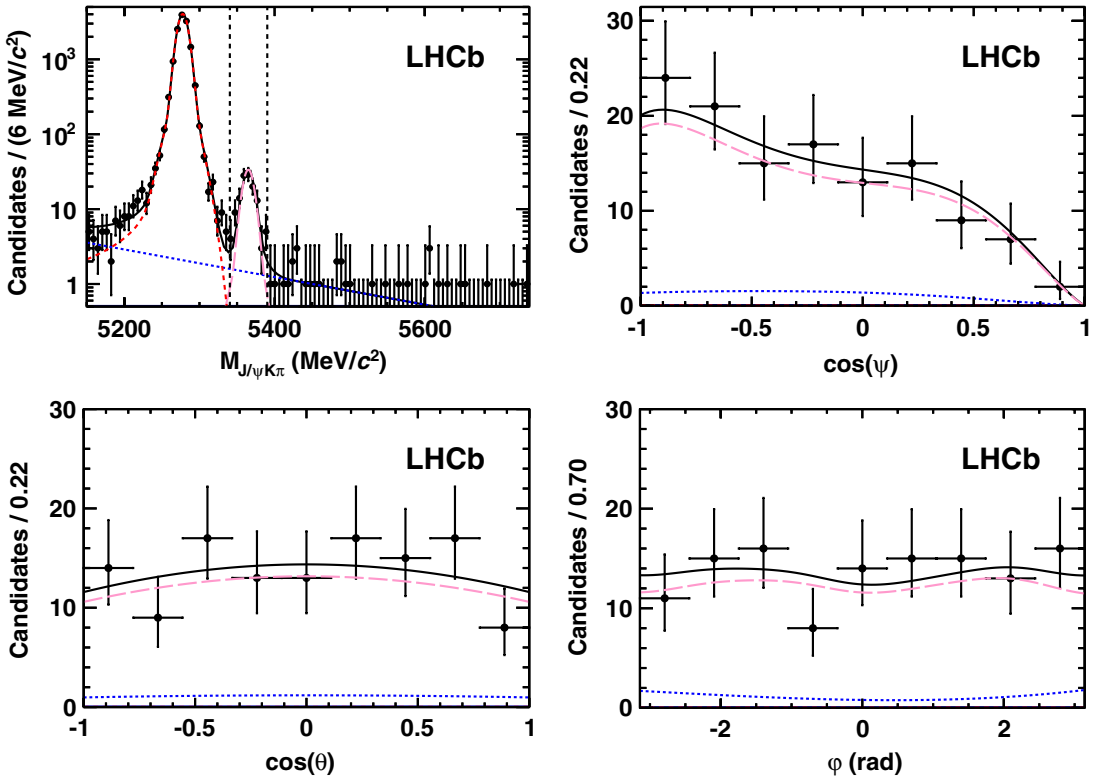

FIG. 3 (color online). Projections of the fit in $M_{J/\psi K\pi}$ and in the angular variables for the mass range indicated by the two dashed vertical lines in the mass plot. The red dashed, pink long-dashed, and blue dotted lines represent the fitted contributions from $B^0 \to J/\psi K^{*0}$, $B^0_s \to J/\psi \bar{K}^{*0}$, and background. The black solid line is their sum.

TABLE I. Summary of the measured $B_s^0 \to J/\psi \bar{K}^{*0}$ angular properties and their statistical and systematic uncertainties.

Parameter name	$\lvert A_S\rvert^2$	f_L	$f_\parallel$
Value and statistical error	$0.07^{+0.15}_{-0.07}$	0.50 ± 0.08	$0.19^{+0.10}_{-0.08}$
Systematic uncertainties			
Angular acceptance	0.044	0.011	0.016
Background angular model	0.038	0.017	0.013
Assumption $\delta_S(M_{K\pi}) =$ constant	0.026	0.005	0.002
B^0 contamination	0.036	0.004	0.007
Fit bias	...	...	0.005
Total systematic error	0.073	0.021	0.022

TABLE II. Angular parameters of $B^0 \to J/\psi K^{*0}$ needed to compute $\mathcal{B}(B_s^0 \to J/\psi \bar{K}^{*0})$. The systematic uncertainties from background modeling and the mass PDF are found to be negligible in this case.

Parameter name	$\lvert A_S\rvert^2$	f_L	$f_\parallel$
Value and statistical error	0.037 ± 0.010	0.569 ± 0.007	0.240 ± 0.009
Systematic uncertainties			
Angular acceptance	0.044	0.011	0.016
Assumption $\delta_S(M_{K\pi}) =$ constant	0.026	0.005	0.002
Total systematic error	0.051	0.012	0.016

The ratio of the two branching fractions is obtained from

$$\frac{\mathcal{B}(B_s^0 \to J/\psi \bar{K}^{*0})}{\mathcal{B}(B^0 \to J/\psi K^{*0})} = \frac{f_d}{f_s} \frac{\varepsilon^{\rm tot}_{B^0}}{\varepsilon^{\rm tot}_{B_s^0}} \frac{\lambda_{B^0}}{\lambda_{B_s^0}} \frac{f^{(d)}_{K^{*0}}}{f^{(s)}_{K^{*0}}} \frac{N_{B_s^0}}{N_{B^0}}, \qquad (5)$$

where f_d (f_s) is the probability of the b quark to hadronize to B^0 (B_s^0) mesons, $\varepsilon^{\rm tot}_{B^0}/\varepsilon^{\rm tot}_{B_s^0}$ is the efficiency ratio, $\lambda_{B^0}/\lambda_{B_s^0}$ is the ratio of angular corrections, $f^{(s)}_{K^{*0}}/f^{(d)}_{K^{*0}}$ is the ratio of K^{*0} fractions, and $N_{B_s^0}/N_{B^0}$ is the ratio of signal yields. The value of f_d/f_s has been taken from Ref. [20]. The efficiencies in the ratio $\varepsilon^{\rm tot}_{B^0}/\varepsilon^{\rm tot}_{B_s^0}$ are computed using simulation and receive two contributions: the efficiency of the offline reconstruction (including geometrical acceptance) and selection cuts, and the trigger efficiency on events that satisfy the analysis offline selection criteria. The systematic uncertainty in the efficiency ratio is negligible due to the similarity of the final states. Effects due to possible differences in the decay time acceptance between data and simulation were found to affect the efficiency ratio by less than 1 per mil. On the other hand, since the efficiency depends on the angular distribution of the decay products, correction factors λ_{B^0} and $\lambda_{B_s^0}$ are applied to account for the difference between the angular amplitudes used in simulation and those measured in the data. The observed numbers of B^0 and B_s^0 decays, denoted by N_{B^0} and $N_{B_s^0}$, correspond to the number of $B_s^0 \to J/\psi K\pi$ and $B^0 \to J/\psi K\pi$ decays with a $K\pi$ mass in a ± 40 MeV/c^2 window around the nominal K^{*0} mass. This includes mostly the K^{*0} meson, but also an S-wave component and the interference between the S-wave and P-wave components. The fraction of candidates with a K^{*0} meson present is then

$$f_{K^{*0}} = \frac{\int_\Omega \mathrm{Acc}(\Omega) \frac{\mathrm{d}^3\Gamma}{\mathrm{d}\Omega}|_{|A_S|=0} \mathrm{d}\Omega}{\int_\Omega \mathrm{Acc}(\Omega) \frac{\mathrm{d}^3\Gamma}{\mathrm{d}\Omega}\, \mathrm{d}\Omega}, \qquad (6)$$

from which the ratio $f^{(s)}_{K^{*0}}/f^{(d)}_{K^{*0}} = 1.09 \pm 0.08$ follows. Table III summarizes all the numbers needed to compute the ratio of branching fractions

TABLE III. Parameter values and errors for $\frac{\mathcal{B}(B_s^0 \to J/\psi \bar{K}^{*0})}{\mathcal{B}(B^0 \to J/\psi K^{*0})}$.

Parameter	Name	Value
Hadronization fractions	f_d/f_s	3.75 ± 0.29
Efficiency ratio	$\varepsilon^{\rm tot}_{B^0}/\varepsilon^{\rm tot}_{B_s^0}$	0.97 ± 0.01
Angular corrections	$\lambda_{B^0}/\lambda_{B_s^0}$	1.01 ± 0.04
Ratio of K^{*0} fractions	$f^{(s)}_{K^{*0}}/f^{(d)}_{K^{*0}}$	1.09 ± 0.08
B signal yields	$N_{B_s^0}/N_{B^0}$	$(8.5^{+0.9}_{-0.8} \pm 0.8) \times 10^{-3}$

$$\frac{\mathcal{B}(B_s^0 \to J/\psi \bar{K}^{*0})}{\mathcal{B}(B^0 \to J/\psi K^{*0})} = (3.43^{+0.34}_{-0.36} \pm 0.50)\%.$$

The contributions to the systematic uncertainty are also listed in Table III and their relative magnitudes are 1.2% for the error in the efficiency ratio; 2.5% for the uncertainty on the transition point (α) of the crystal ball function; 8.6% for the parametrization of the upper tail of the B^0 peak; 3.9% for the angular correction of the efficiencies; 7.3% for the uncertainty on the ratio $f_{K^{*0}}^{(s)}/f_{K^{*0}}^{(d)}$; and 7.7% for the uncertainty on f_d/f_s. The errors are added in quadrature.

Taking the value $\mathcal{B}(B^0 \to J/\psi K^{*0}) = (1.29 \pm 0.05 \pm 0.13) \times 10^{-3}$ from Ref. [4] the following branching fraction is obtained:

$$\mathcal{B}(B_s^0 \to J/\psi \bar{K}^{*0}) = (4.4^{+0.5}_{-0.4} \pm 0.8) \times 10^{-5}.$$

This value is compatible with the CDF measurement [2] and is similar to the naive quark spectator model prediction of Eq. (1), although it is closer to the estimation in Ref. [1], $\mathcal{B}(B_s^0 \to J/\psi \bar{K}^{*0}) \sim 2 \times \mathcal{B}(B_d^0 \to J/\psi \rho^0) = (4.6 \pm 0.4) \times 10^{-5}$. The branching fraction measured here is, in fact, the average of the $B_s^0 \to J/\psi \bar{K}^{*0}$ and $\bar{B}_s^0 \to J/\psi K^{*0}$ branching fractions and corresponds to the time integrated quantity, while theory predictions usually refer to the branching fraction at $t = 0$ [21]. In the case of $B_s^0 \to J/\psi \bar{K}^{*0}$, the two differ by $(\Delta\Gamma_s/2\Gamma_s)^2 = (0.77 \pm 0.25)\%$, where $\Delta\Gamma_s = \Gamma_L - \Gamma_H$, $\Gamma_s = (\Gamma_L + \Gamma_H)/2$, and $\Gamma_{L(H)}$ is the decay width of the light (heavy) B_s^0-mass eigenstate.

In conclusion, using 0.37 fb^{-1} of pp collisions collected by the LHCb detector at $\sqrt{s} = 7$ TeV, a measurement of the $B_s^0 \to J/\psi \bar{K}^{*0}$ branching fraction yields $\mathcal{B}(B_s^0 \to J/\psi \bar{K}^{*0}) = (4.4^{+0.5}_{-0.4} \pm 0.8) \times 10^{-5}$. In addition, an angular analysis of the decay products is presented, which provides the first measurement of the K^{*0} polarization fractions in this decay, giving $f_L = 0.50 \pm 0.08 \pm 0.02$, $f_\parallel = 0.19^{+0.10}_{-0.08} \pm 0.02$, and an S-wave contribution of $|A_S|^2 = 0.07^{+0.15}_{-0.07}$ in a ± 40 MeV$/c^2$ window around the K^{*0} mass.

We express our gratitude to our colleagues in the CERN accelerator departments for the excellent performance of the LHC. We thank the technical and administrative staff at CERN and at the LHCb institutes, and acknowledge support from the National Agencies: CAPES, CNPq, FAPERJ, and FINEP (Brazil); CERN; NSFC (China); CNRS/IN2P3 (France); BMBF, DFG, HGF, and MPG (Germany); SFI (Ireland); INFN (Italy); FOM and NWO (The Netherlands); SCSR (Poland); ANCS (Romania); MinES of Russia and Rosatom (Russia); MICINN, XuntaGal and GENCAT (Spain); SNSF and SER (Switzerland); NAS Ukraine (Ukraine); STFC (United Kingdom); NSF (USA). We also acknowledge the support received from the ERC under FP7 and the Region Auvergne.

[1] S. Faller, R. Fleischer, and T. Mannel, Phys. Rev. D **79**, 014005 (2009).
[2] T. Aaltonen *et al.* (CDF Collaboration), Phys. Rev. D **83**, 052012 (2011).
[3] K. Nakamura *et al.* (Particle Data Group), J. Phys. G **37**, 075021 (2010).
[4] K. Abe *et al.* (Belle Collaboration), Phys. Lett. B **538**, 11 (2002).
[5] A. A. Alves, Jr. *et al.* (LHCb Collaboration), JINST **3**, S08005 (2008).
[6] T. Sjöstrand, S. Mrenna, and P. Skands, J. High Energy Phys. 05 (2006) 026.
[7] I. Belyaev *et al.*, Nuclear Science Symposium Conference Record (NSS/MIC) **IEEE**, 1155 (2010).
[8] D. J. Lange, Nucl. Instrum. Methods Phys. Res., Sect. A **462**, 152 (2001).
[9] P. Golonka and Z. Was, Eur. Phys. J. C **45**, 97 (2006).
[10] J. Allison *et al.* (GEANT4 Collaboration), Nucl. Sci. J. **53**, 270 (2006); S. Agostinelli *et al.* (GEANT4 Collaboration), Nucl. Instrum. Methods Phys. Res., Sect. A **506**, 250 (2003).
[11] M. Clemencic, G. Corti, S. Easo, C. R. Jones, S. Miglioranzi, M. Pappagallo, and P. Robbe, J. Phys. Conf. Ser. **331**, 032023 (2011).
[12] D. Martínez Santos, PhD thesis, University of Santiago de Compostela, 2010, Report No. CERN-THESIS-2010-068.
[13] D. Karlen, Comput. Phys. **12**, 380 (1998).
[14] B. Aubert *et al.* (*BABAR* Collaboration), Phys. Rev. D **79**, 112001 (2009).
[15] T. Skwarnicki, Ph.D. thesis, Institute of Nuclear Physics, Krakow, 1986, Report No. DESY-F31-86-02.
[16] R. Aaij *et al.* (LHCb Collaboration), Phys. Lett. B **708**, 241 (2012).
[17] B. Aubert *et al.* (*BABAR* Collaboration), Phys. Rev. D **71**, 032005 (2005).
[18] T. Aaltonen *et al.* (CDF Collaboration), CDF public note Report No. 8950, 2011.
[19] T. du Pree, Ph.D. thesis, Vrije Universiteit (Amsterdam), 2010, Report No. CERN-THESIS-2010-124.
[20] R. Aaij *et al.* (LHCb Collaboration), Phys. Rev. D **85**, 032008 (2012).
[21] K. De Bruyn, R. Fleischer, R. Knegjens, P. Koppenburg, M. Merk, and N. Tuning, Phys. Rev. D **86**, 014027 (2012).

R. Aaij,[38] C. Abellan Beteta,[33,a] A. Adametz,[11] B. Adeva,[34] M. Adinolfi,[43] C. Adrover,[6] A. Affolder,[49] Z. Ajaltouni,[5] J. Albrecht,[35] F. Alessio,[35] M. Alexander,[48] S. Ali,[38] G. Alkhazov,[27] P. Alvarez Cartelle,[34] A. A. Alves, Jr.,[22] S. Amato,[2] Y. Amhis,[36] J. Anderson,[37] R. B. Appleby,[51] O. Aquines Gutierrez,[10] F. Archilli,[18,35] A. Artamonov,[32] M. Artuso,[53,35] E. Aslanides,[6] G. Auriemma,[22,b] S. Bachmann,[11] J. J. Back,[45] V. Balagura,[28,35] W. Baldini,[16] R. J. Barlow,[51] C. Barschel,[35] S. Barsuk,[7] W. Barter,[44] A. Bates,[48] C. Bauer,[10] Th. Bauer,[38] A. Bay,[36] J. Beddow,[48] I. Bediaga,[1] S. Belogurov,[28] K. Belous,[32] I. Belyaev,[28] E. Ben-Haim,[8] M. Benayoun,[8] G. Bencivenni,[18] S. Benson,[47] J. Benton,[43] R. Bernet,[37] M.-O. Bettler,[17] M. van Beuzekom,[38] A. Bien,[11] S. Bifani,[12] T. Bird,[51] A. Bizzeti,[17,c] P. M. Bjørnstad,[51] T. Blake,[35] F. Blanc,[36] C. Blanks,[50] J. Blouw,[11] S. Blusk,[53] A. Bobrov,[31] V. Bocci,[22] A. Bondar,[31] N. Bondar,[27] W. Bonivento,[15] S. Borghi,[48,51] A. Borgia,[53] T. J. V. Bowcock,[49] C. Bozzi,[16] T. Brambach,[9] J. van den Brand,[39] J. Bressieux,[36] D. Brett,[51] M. Britsch,[10] T. Britton,[53] N. H. Brook,[43] H. Brown,[49] A. Büchler-Germann,[37] I. Burducea,[26] A. Bursche,[37] J. Buytaert,[35] S. Cadeddu,[15] O. Callot,[7] M. Calvi,[20,d] M. Calvo Gomez,[33,a] A. Camboni,[33] P. Campana,[18,35] A. Carbone,[14] G. Carboni,[21,e] R. Cardinale,[19,35,f] A. Cardini,[15] L. Carson,[50] K. Carvalho Akiba,[2] G. Casse,[49] M. Cattaneo,[35] Ch. Cauet,[9] M. Charles,[52] Ph. Charpentier,[35] P. Chen,[3,36] N. Chiapolini,[37] M. Chrzaszcz,[23] K. Ciba,[35] X. Cid Vidal,[34] G. Ciezarek,[50] P. E. L. Clarke,[47] M. Clemencic,[35] H. V. Cliff,[44] J. Closier,[35] C. Coca,[26] V. Coco,[38] J. Cogan,[6] E. Cogneras,[5] P. Collins,[35] A. Comerma-Montells,[33] A. Contu,[52] A. Cook,[43] M. Coombes,[43] G. Corti,[35] B. Couturier,[35] G. A. Cowan,[36] D. Craik,[45] R. Currie,[47] C. D'Ambrosio,[35] P. David,[8] P. N. Y. David,[38] I. De Bonis,[4] K. De Bruyn,[38] S. De Capua,[21,e] M. De Cian,[37] J. M. De Miranda,[1] L. De Paula,[2] P. De Simone,[18] D. Decamp,[4] M. Deckenhoff,[9] H. Degaudenzi,[36,35] L. Del Buono,[8] C. Deplano,[15] D. Derkach,[14,35] O. Deschamps,[5] F. Dettori,[39] J. Dickens,[44] H. Dijkstra,[35] P. Diniz Batista,[1] F. Domingo Bonal,[33,a] S. Donleavy,[49] F. Dordei,[11] A. Dosil Suárez,[34] D. Dossett,[45] A. Dovbnya,[40] F. Dupertuis,[36] R. Dzhelyadin,[32] A. Dziurda,[23] A. Dzyuba,[27] S. Easo,[46] U. Egede,[50] V. Egorychev,[28] S. Eidelman,[31] D. van Eijk,[38] F. Eisele,[11] S. Eisenhardt,[47] R. Ekelhof,[9] L. Eklund,[48] I. El Rifai,[5] Ch. Elsasser,[37] D. Elsby,[42] D. Esperante Pereira,[34] A. Falabella,[16,14,g] C. Färber,[11] G. Fardell,[47] C. Farinelli,[38] S. Farry,[12] V. Fave,[36] V. Fernandez Albor,[34] F. Ferreira Rodrigues,[1] M. Ferro-Luzzi,[35] S. Filippov,[30] C. Fitzpatrick,[47] M. Fontana,[10] F. Fontanelli,[19,f] R. Forty,[35] O. Francisco,[2] M. Frank,[35] C. Frei,[35] M. Frosini,[17,h] S. Furcas,[20] A. Gallas Torreira,[34] D. Galli,[14,i] M. Gandelman,[2] P. Gandini,[52] Y. Gao,[3] J-C. Garnier,[35] J. Garofoli,[53] J. Garra Tico,[44] L. Garrido,[33] D. Gascon,[33] C. Gaspar,[35] R. Gauld,[52] N. Gauvin,[36] E. Gersabeck,[11] M. Gersabeck,[35] T. Gershon,[45,35] Ph. Ghez,[4] V. Gibson,[44] V. V. Gligorov,[35] C. Göbel,[54] D. Golubkov,[28] A. Golutvin,[50,28,35] A. Gomes,[2] H. Gordon,[52] M. Grabalosa Gándara,[33] R. Graciani Diaz,[33] L. A. Granado Cardoso,[35] E. Graugés,[33] G. Graziani,[17] A. Grecu,[26] E. Greening,[52] S. Gregson,[44] O. Grünberg,[55] B. Gui,[53] E. Gushchin,[30] Yu. Guz,[32] T. Gys,[35] C. Hadjivasiliou,[53] G. Haefeli,[36] C. Haen,[35] S. C. Haines,[44] T. Hampson,[43] S. Hansmann-Menzemer,[11] N. Harnew,[52] S. T. Harnew,[43] J. Harrison,[51] P. F. Harrison,[45] T. Hartmann,[55] J. He,[7] V. Heijne,[38] K. Hennessy,[49] P. Henrard,[5] J. A. Hernando Morata,[34] E. van Herwijnen,[35] E. Hicks,[49] M. Hoballah,[5] P. Hopchev,[4] W. Hulsbergen,[38] P. Hunt,[52] T. Huse,[49] R. S. Huston,[12] D. Hutchcroft,[49] D. Hynds,[48] V. Iakovenko,[41] P. Ilten,[12] J. Imong,[43] R. Jacobsson,[35] A. Jaeger,[11] M. Jahjah Hussein,[5] E. Jans,[38] F. Jansen,[38] P. Jaton,[36] B. Jean-Marie,[7] F. Jing,[3] M. John,[52] D. Johnson,[52] C. R. Jones,[44] B. Jost,[35] M. Kaballo,[9] S. Kandybei,[40] M. Karacson,[35] T. M. Karbach,[9] J. Keaveney,[12] I. R. Kenyon,[42] U. Kerzel,[35] T. Ketel,[39] A. Keune,[36] B. Khanji,[6] Y. M. Kim,[47] M. Knecht,[36] O. Kochebina,[7] I. Komarov,[29] R. F. Koopman,[39] P. Koppenburg,[38] M. Korolev,[29] A. Kozlinskiy,[38] L. Kravchuk,[30] K. Kreplin,[11] M. Kreps,[45] G. Krocker,[11] P. Krokovny,[31] F. Kruse,[9] M. Kucharczyk,[20,23,35,d] V. Kudryavtsev,[31] T. Kvaratskheliya,[28,35] V. N. La Thi,[36] D. Lacarrere,[35] G. Lafferty,[51] A. Lai,[15] D. Lambert,[47] R. W. Lambert,[39] E. Lanciotti,[35] G. Lanfranchi,[18] C. Langenbruch,[35] T. Latham,[45] C. Lazzeroni,[42] R. Le Gac,[6] J. van Leerdam,[38] J.-P. Lees,[4] R. Lefèvre,[5] A. Leflat,[29,35] J. Lefrançois,[7] O. Leroy,[6] T. Lesiak,[23] L. Li,[3] Y. Li,[3] L. Li Gioi,[5] M. Lieng,[9] M. Liles,[49] R. Lindner,[35] C. Linn,[11] B. Liu,[3] G. Liu,[35] J. von Loeben,[20] J. H. Lopes,[2] E. Lopez Asamar,[33] N. Lopez-March,[36] H. Lu,[3] J. Luisier,[36] A. Mac Raighne,[48] F. Machefert,[7] I. V. Machikhiliyan,[4,28] F. Maciuc,[10] O. Maev,[27,35] J. Magnin,[1] S. Malde,[52] R. M. D. Mamunur,[35] G. Manca,[15,j] G. Mancinelli,[6] N. Mangiafave,[44] U. Marconi,[14] R. Märki,[36] J. Marks,[11] G. Martellotti,[22] A. Martens,[8] L. Martin,[52] A. Martín Sánchez,[7] M. Martinelli,[38] D. Martinez Santos,[35] A. Massafferri,[1] Z. Mathe,[12] C. Matteuzzi,[20] M. Matveev,[27] E. Maurice,[6] A. Mazurov,[16,30,35] J. McCarthy,[42] G. McGregor,[51] R. McNulty,[12] M. Meissner,[11] M. Merk,[38] J. Merkel,[9] D. A. Milanes,[13] M.-N. Minard,[4] J. Molina Rodriguez,[54] S. Monteil,[5] D. Moran,[12] P. Morawski,[23] R. Mountain,[53] I. Mous,[38] F. Muheim,[47] K. Müller,[37] R. Muresan,[26] B. Muryn,[24] B. Muster,[36] J. Mylroie-Smith,[49] P. Naik,[43] T. Nakada,[36] R. Nandakumar,[46] I. Nasteva,[1] M. Needham,[47] N. Neufeld,[35] A. D. Nguyen,[36] C. Nguyen-Mau,[36,k] M. Nicol,[7] V. Niess,[5] N. Nikitin,[29] T. Nikodem,[11]

A. Nomerotski,[52,35] A. Novoselov,[32] A. Oblakowska-Mucha,[24] V. Obraztsov,[32] S. Oggero,[38] S. Ogilvy,[48] O. Okhrimenko,[41] R. Oldeman,[15,35,j] M. Orlandea,[26] J. M. Otalora Goicochea,[2] P. Owen,[50] B. K. Pal,[53] A. Palano,[13,l] M. Palutan,[18] J. Panman,[35] A. Papanestis,[46] M. Pappagallo,[48] C. Parkes,[51] C. J. Parkinson,[50] G. Passaleva,[17] G. D. Patel,[49] M. Patel,[50] G. N. Patrick,[46] C. Patrignani,[19,f] C. Pavel-Nicorescu,[26] A. Pazos Alvarez,[34] A. Pellegrino,[38] G. Penso,[22,m] M. Pepe Altarelli,[35] S. Perazzini,[14,i] D. L. Perego,[20,d] E. Perez Trigo,[34] A. Pérez-Calero Yzquierdo,[33] P. Perret,[5] M. Perrin-Terrin,[6] G. Pessina,[20] A. Petrolini,[19,f] A. Phan,[53] E. Picatoste Olloqui,[33] B. Pie Valls,[33] B. Pietrzyk,[4] T. Pilař,[45] D. Pinci,[22] S. Playfer,[47] M. Plo Casasus,[34] F. Polci,[8] G. Polok,[23] A. Poluektov,[45,31] E. Polycarpo,[2] D. Popov,[10] B. Popovici,[26] C. Potterat,[33] A. Powell,[52] J. Prisciandaro,[36] V. Pugatch,[41] A. Puig Navarro,[33] W. Qian,[53] J. H. Rademacker,[43] B. Rakotomiaramanana,[36] M. S. Rangel,[2] I. Raniuk,[40] N. Rauschmayr,[35] G. Raven,[39] S. Redford,[52] M. M. Reid,[45] A. C. dos Reis,[1] S. Ricciardi,[46] A. Richards,[50] K. Rinnert,[49] D. A. Roa Romero,[5] P. Robbe,[7] E. Rodrigues,[48,51] F. Rodrigues,[2] P. Rodriguez Perez,[34] G. J. Rogers,[44] S. Roiser,[35] V. Romanovsky,[32] A. Romero Vidal,[34] M. Rosello,[33,a] J. Rouvinet,[36] T. Ruf,[35] H. Ruiz,[33] G. Sabatino,[21,e] J. J. Saborido Silva,[34] N. Sagidova,[27] P. Sail,[48] B. Saitta,[15,j] C. Salzmann,[37] B. Sanmartin Sedes,[34] M. Sannino,[19,f] R. Santacesaria,[22] C. Santamarina Rios,[34] R. Santinelli,[35] E. Santovetti,[21,e] M. Sapunov,[6] A. Sarti,[18,m] C. Satriano,[22,b] A. Satta,[21] M. Savrie,[16,g] D. Savrina,[28] P. Schaack,[50] M. Schiller,[39] H. Schindler,[35] S. Schleich,[9] M. Schlupp,[9] M. Schmelling,[10] B. Schmidt,[35] O. Schneider,[36] A. Schopper,[35] M.-H. Schune,[7] R. Schwemmer,[35] B. Sciascia,[18] A. Sciubba,[18,m] M. Seco,[34] A. Semennikov,[28] K. Senderowska,[24] I. Sepp,[50] N. Serra,[37] J. Serrano,[6] P. Seyfert,[11] M. Shapkin,[32] I. Shapoval,[40,35] P. Shatalov,[28] Y. Shcheglov,[27] T. Shears,[49] L. Shekhtman,[31] O. Shevchenko,[40] V. Shevchenko,[28] A. Shires,[50] R. Silva Coutinho,[45] T. Skwarnicki,[53] N. A. Smith,[49] E. Smith,[52,46] M. Smith,[51] K. Sobczak,[5] F. J. P. Soler,[48] A. Solomin,[43] F. Soomro,[18,35] D. Souza,[43] B. Souza De Paula,[2] B. Spaan,[9] A. Sparkes,[47] P. Spradlin,[48] F. Stagni,[35] S. Stahl,[11] O. Steinkamp,[37] S. Stoica,[26] S. Stone,[53,35] B. Storaci,[38] M. Straticiuc,[26] U. Straumann,[37] V. K. Subbiah,[35] S. Swientek,[9] M. Szczekowski,[25] P. Szczypka,[36] T. Szumlak,[24] S. T'Jampens,[4] M. Teklishyn,[7] E. Teodorescu,[26] F. Teubert,[35] C. Thomas,[52] E. Thomas,[35] J. van Tilburg,[11] V. Tisserand,[4] M. Tobin,[37] S. Tolk,[39] S. Topp-Joergensen,[52] N. Torr,[52] E. Tournefier,[4,50] S. Tourneur,[36] M. T. Tran,[36] A. Tsaregorodtsev,[6] N. Tuning,[38] M. Ubeda Garcia,[35] A. Ukleja,[25] U. Uwer,[11] V. Vagnoni,[14] G. Valenti,[14] R. Vazquez Gomez,[33] P. Vazquez Regueiro,[34] S. Vecchi,[16] J. J. Velthuis,[43] M. Veltri,[17,n] G. Veneziano,[36] M. Vesterinen,[35] B. Viaud,[7] I. Videau,[7] D. Vieira,[2] X. Vilasis-Cardona,[33,a] J. Visniakov,[34] A. Vollhardt,[37] D. Volyanskyy,[10] D. Voong,[43] A. Vorobyev,[27] V. Vorobyev,[31] C. Voß,[55] H. Voss,[10] R. Waldi,[55] R. Wallace,[12] S. Wandernoth,[11] J. Wang,[53] D. R. Ward,[44] N. K. Watson,[42] A. D. Webber,[51] D. Websdale,[50] M. Whitehead,[45] J. Wicht,[35] D. Wiedner,[11] L. Wiggers,[38] G. Wilkinson,[52] M. P. Williams,[45,46] M. Williams,[50] F. F. Wilson,[46] J. Wishahi,[9] M. Witek,[23] W. Witzeling,[35] S. A. Wotton,[44] S. Wright,[44] S. Wu,[3] K. Wyllie,[35] Y. Xie,[47] F. Xing,[52] Z. Xing,[53] Z. Yang,[3] R. Young,[47] X. Yuan,[3] O. Yushchenko,[32] M. Zangoli,[14] M. Zavertyaev,[10,o] F. Zhang,[3] L. Zhang,[53] W. C. Zhang,[12] Y. Zhang,[3] A. Zhelezov,[11] L. Zhong,[3] and A. Zvyagin[35]

(LHCb Collaboration)

[1]*Centro Brasileiro de Pesquisas Físicas (CBPF), Rio de Janeiro, Brazil*
[2]*Universidade Federal do Rio de Janeiro (UFRJ), Rio de Janeiro, Brazil*
[3]*Center for High Energy Physics, Tsinghua University, Beijing, China*
[4]*LAPP, Université de Savoie, CNRS/IN2P3, Annecy-Le-Vieux, France*
[5]*Clermont Université, Université Blaise Pascal, CNRS/IN2P3, LPC, Clermont-Ferrand, France*
[6]*CPPM, Aix-Marseille Université, CNRS/IN2P3, Marseille, France*
[7]*LAL, Université Paris-Sud, CNRS/IN2P3, Orsay, France*
[8]*LPNHE, Université Pierre et Marie Curie, Université Paris Diderot, CNRS/IN2P3, Paris, France*
[9]*Fakultät Physik, Technische Universität Dortmund, Dortmund, Germany*
[10]*Max-Planck-Institut für Kernphysik (MPIK), Heidelberg, Germany*
[11]*Physikalisches Institut, Ruprecht-Karls-Universität Heidelberg, Heidelberg, Germany*
[12]*School of Physics, University College Dublin, Dublin, Ireland*
[13]*Sezione INFN di Bari, Bari, Italy*
[14]*Sezione INFN di Bologna, Bologna, Italy*
[15]*Sezione INFN di Cagliari, Cagliari, Italy*
[16]*Sezione INFN di Ferrara, Ferrara, Italy*
[17]*Sezione INFN di Firenze, Firenze, Italy*
[18]*Laboratori Nazionali dell'INFN di Frascati, Frascati, Italy*

[19]*Sezione INFN di Genova, Genova, Italy*
[20]*Sezione INFN di Milano Bicocca, Milano, Italy*
[21]*Sezione INFN di Roma Tor Vergata, Roma, Italy*
[22]*Sezione INFN di Roma La Sapienza, Roma, Italy*
[23]*Henryk Niewodniczanski Institute of Nuclear Physics Polish Academy of Sciences, Kraków, Poland*
[24]*AGH University of Science and Technology, Kraków, Poland*
[25]*Soltan Institute for Nuclear Studies, Warsaw, Poland*
[26]*Horia Hulubei National Institute of Physics and Nuclear Engineering, Bucharest-Magurele, Romania*
[27]*Petersburg Nuclear Physics Institute (PNPI), Gatchina, Russia*
[28]*Institute of Theoretical and Experimental Physics (ITEP), Moscow, Russia*
[29]*Institute of Nuclear Physics, Moscow State University (SINP MSU), Moscow, Russia*
[30]*Institute for Nuclear Research of the Russian Academy of Sciences (INR RAN), Moscow, Russia*
[31]*Budker Institute of Nuclear Physics (SB RAS) and Novosibirsk State University, Novosibirsk, Russia*
[32]*Institute for High Energy Physics (IHEP), Protvino, Russia*
[33]*Universitat de Barcelona, Barcelona, Spain*
[34]*Universidad de Santiago de Compostela, Santiago de Compostela, Spain*
[35]*European Organization for Nuclear Research (CERN), Geneva, Switzerland*
[36]*Ecole Polytechnique Fédérale de Lausanne (EPFL), Lausanne, Switzerland*
[37]*Physik-Institut, Universität Zürich, Zürich, Switzerland*
[38]*Nikhef National Institute for Subatomic Physics, Amsterdam, The Netherlands*
[39]*Nikhef National Institute for Subatomic Physics and VU University Amsterdam, Amsterdam, The Netherlands*
[40]*NSC Kharkiv Institute of Physics and Technology (NSC KIPT), Kharkiv, Ukraine*
[41]*Institute for Nuclear Research of the National Academy of Sciences (KINR), Kyiv, Ukraine*
[42]*University of Birmingham, Birmingham, United Kingdom*
[43]*H.H. Wills Physics Laboratory, University of Bristol, Bristol, United Kingdom*
[44]*Cavendish Laboratory, University of Cambridge, Cambridge, United Kingdom*
[45]*Department of Physics, University of Warwick, Coventry, United Kingdom*
[46]*STFC Rutherford Appleton Laboratory, Didcot, United Kingdom*
[47]*School of Physics and Astronomy, University of Edinburgh, Edinburgh, United Kingdom*
[48]*School of Physics and Astronomy, University of Glasgow, Glasgow, United Kingdom*
[49]*Oliver Lodge Laboratory, University of Liverpool, Liverpool, United Kingdom*
[50]*Imperial College London, London, United Kingdom*
[51]*School of Physics and Astronomy, University of Manchester, Manchester, United Kingdom*
[52]*Department of Physics, University of Oxford, Oxford, United Kingdom*
[53]*Syracuse University, Syracuse, New York, USA*
[54]*Pontifícia Universidade Católica do Rio de Janeiro (PUC-Rio), Rio de Janeiro, Brazil [associated with Universidade Federal do Rio de Janeiro (UFRJ), Rio de Janeiro, Brazil]*
[55]*Institut für Physik, Universität Rostock, Rostock, Germany [associated with Physikalisches Institut, Ruprecht-Karls-Universität Heidelberg, Heidelberg, Germany]*

[a]LIFAELS, La Salle, Universitat Ramon Llull, Barcelona, Spain.
[b]Università della Basilicata, Potenza, Italy.
[c]Università di Modena e Reggio Emilia, Modena, Italy.
[d]Università di Milano Bicocca, Milano, Italy.
[e]Università di Roma Tor Vergata, Roma, Italy.
[f]Università di Genova, Genova, Italy.
[g]Università di Ferrara, Ferrara, Italy.
[h]Università di Firenze, Firenze, Italy.
[i]Università di Bologna, Bologna, Italy.
[j]Università di Cagliari, Cagliari, Italy.
[k]Hanoi University of Science, Hanoi, Viet Nam.
[l]Università di Bari, Bari, Italy.
[m]Università di Roma La Sapienza, Roma, Italy.
[n]Università di Urbino, Urbino, Italy.
[o]P.N. Lebedev Physical Institute, Russian Academy of Science (LPI RAS), Moscow, Russia.